AJNR

MR characteristics of histopathologic subtypes of spinal ependymoma.

H Kahan, E M Sklar, M J Post and J H Bruce

AJNR Am J Neuroradiol 1996, 17 (1) 143-150
http://www.ajnr.org/content/17/1/143

MR Characteristics of Histopathologic Subtypes of Spinal Ependymoma

Heather Kahan, Evelyn M. L. Sklar, M. Judith Donovan Post, and Jocelyn H. Bruce

PURPOSE: To examine MR characteristics and enhancement patterns of spinal ependymomas and compare these data with histopathologic subtypes. **METHODS:** The MR images from 26 cases of pathologically proved spinal ependymomas were evaluated with respect to seven criteria: signal characteristics, enhancement pattern, length of involvement, cysts or syrinxes, hemorrhage, bony changes, and type of cord expansion. Signal characteristics were then correlated with histologic subtype. **RESULTS:** In the category of enhancement pattern, our results differed markedly from published data, with only 38% of cases demonstrating classic homogeneous enhancement. The remainder of our cases (62%) demonstrated other enhancement patterns, including heterogeneous (31%), rim (19%), minimal (6%), and no enhancement (6%). Pathologic comparison revealed that one histologic subtype, the myxopapillary ependymoma, demonstrated unique imaging characteristics on T1-weighted images. A highly statistically significant percentage of this variant was hyperintense on T1, whereas most nonmyxopapillary ependymomas were hypointense. **CONCLUSION:** The radiologist should be aware of alternative patterns of enhancement of spinal ependymomas and not be dissuaded from the diagnosis in appropriate clinical settings. In addition, one histologic subtype, myxopapillary, often exhibits signal characteristics different from nonmyxopapillary types, appearing hyperintense on T1 probably because of their intracellular and perivascular accumulation of mucin.

Index terms: Ependymoma; Spinal cord, magnetic resonance; Spinal cord, neoplasms

AJNR Am J Neuroradiol 17:143–150, January 1996

We reviewed the magnetic resonance (MR) images of a large series (N = 26) of surgically proved cases of spinal ependymomas to determine the characteristic imaging patterns and to compare the MR signal characteristics with histopathologic findings.

Materials and Methods

Twenty-six patients with pathologically proved spinal ependymomas were studied retrospectively with MR between December 1986 and December 1993. All examinations were performed on mid- or high-field-strength units and routinely included T1- and T2-weighted sagittal images and T1-weighted and gradient-echo axial projections. Two experienced neuroradiologists analyzed the images and were blinded to the histopathologic subtype. Sixteen of the 26 patients also had contrast-enhanced images. The diagnosis for each patient was documented by surgical pathology. None of the patients was taking steroids at the time the imaging studies were obtained.

Criteria used to evaluate the MR images included type of cord enlargement (symmetric or asymmetric), presence of bone changes, presence and type of cystic components (intratumoral or rostral or caudal cysts) or reactive dilatation of the central canal, evidence of hemorrhage, length of involvement, signal characteristics, and enhancement pattern. When evaluating for signal characteristics, the tumor signal was compared with normal cord signal, and assigned to one of three categories: (*a*) hypointense, (*b*) isointense, or (*c*) hyperintense to normal cord. Each case was then correlated with the histology pattern determined by surgical pathology. When the signal was heterogeneous, the predominant signal was used. For those tumors with cystic components, the signal from the more solid-appearing portions of the lesion was recorded.

Results

Fourteen patients were men and twelve were women. Their ages ranged from 19 to 77 years, with a mean age of 44. Nine ependymomas

Received February 6, 1995; accepted after revision June 26.

From the Department of Radiology, University of Miami (Fla) School of Medicine.

Address reprint requests to Heather Kahan, MD, University of Miami School of Medicine, Department of Radiology (R-308), 1115 NW 14th St, Miami, FL 33136.

AJNR 17:143–150, Jan 1996 0195-6108/96/1701–0143

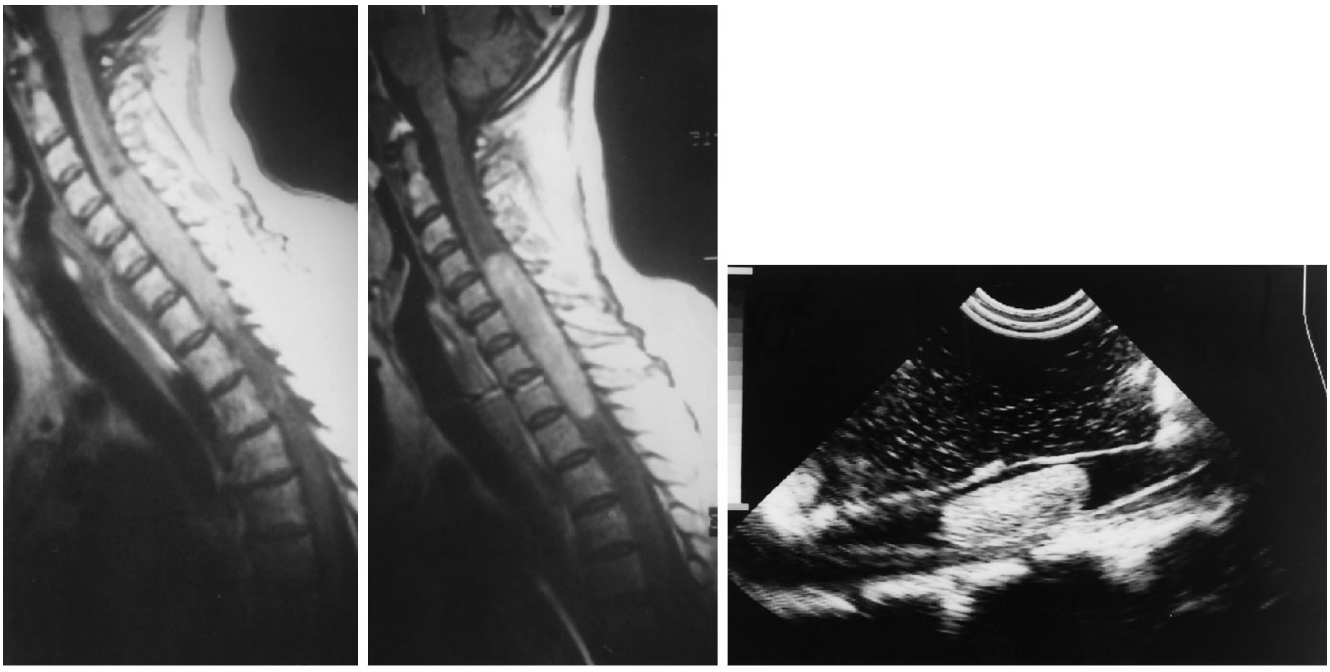

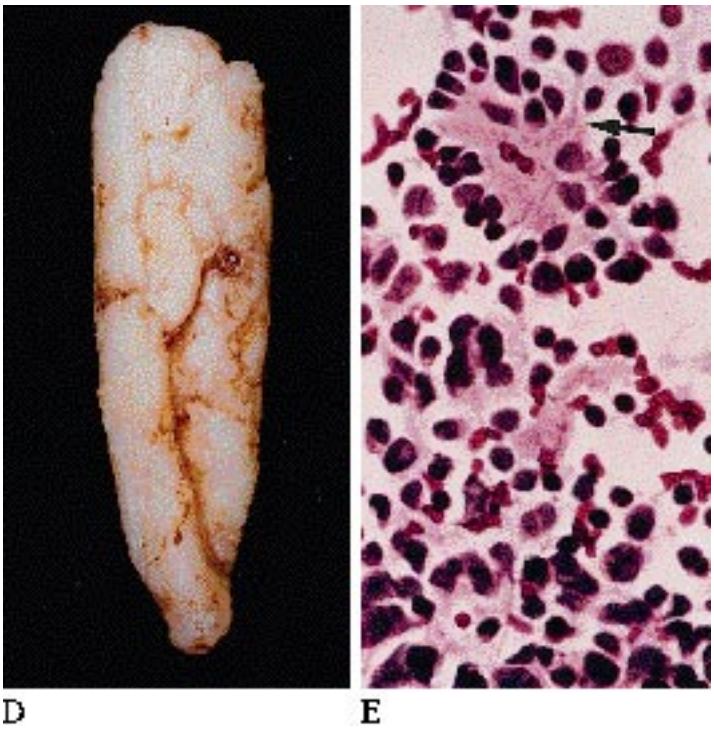

Fig 1. Unenhanced T1-weighted (700/20/2 [repetition time/echo time/excitations]) sagittal image (*A*) demonstrates a large, well-circumscribed cervical cellular ependymoma that markedly enhances with contrast (*B*). Secondary dilatation of the canal is noted both above and below the lesion. This finding was confirmed with intraoperative ultrasound (*C*), and completely resolved after surgery. The excised tumor (*D*) consisted of a well-defined, elongated, firm, and pale tan mass that measured 6.5 × 2.0 × 1.2 cm. The surface was lobulated focally without any significant hypervascularity. Cut sections were smooth, pale tan, and firm in consistency. There was no apparent encapsulation. No evidence of necrosis, hemorrhage, or gritty calcification was noted. Histologic section (*E*) reveals ependymoma cells clustered around small vessels with typical perivascular anuclear zone, forming small rosettes (*arrow*) (hematoxylin-eosin stain, magnification ×400).

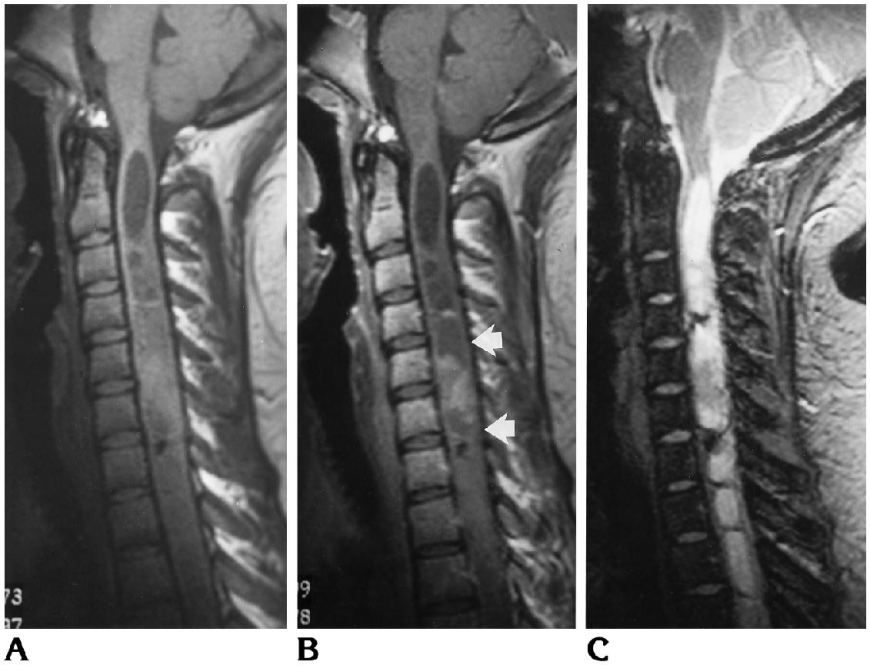

Fig 2. T1-weighted (600/20/2) sagittal image (*A*) demonstrates a cellular ependymoma of the cervical cord, with intratumoral cysts best delineated on the enhanced study (550/25/2) (*B*). The *arrows* show the true intratumoral cysts to be surrounded by enhancement. The T2-weighted (1500/80/2) sagittal image (*C*) shows a heterogeneous hyperintense lesion throughout the cervical cord. Areas of focal hypointensity most likely represent areas of hemosiderin deposition, also seen on *A* and *B*.

occurred in the cervical spine, whereas 1 occurred at the cervicothoracic junction, 2 in the thoracic, 2 at the thoracolumbar junction, and 12 in the lumbosacral spine.

Concerning our imaging results, 14 (100%) of 14 cervical and thoracic ependymomas caused symmetric expansion of the spinal cord. Three (11.5%) of 26 cases had recognizable osseous changes on MR. These changes included bone remodeling, erosion, and scalloping of the posterior vertebral bodies. All of those changes involved the lumbar and lumbosacral spine. Sixteen (61.5%) of 26 cases had associated cysts. Eight (30.1%) of 26 of our cases demonstrated intratumoral cysts, whereas 6 (23%) of 26 showed rostral or caudal cysts, and 9 (34.6%) of 26 cases had secondary reactive dilatation of the central canal (Figs 1, 2, and 3). Some patients demonstrated more than one type of cystic change. These three types of cystic change will be more fully characterized in the "Discussion." With regard to hemorrhage, 5 (19%) of 26 cases demonstrated areas of chronic hemorrhage on MR images (Fig 4). The category of extent of involvement yielded a range of 1 to 17 vertebral segments, with a mean of 4.5. With regard to signal characteristics, 22 (77%) of 26 cases were isointense or hypointense on T1-weighted sequences, whereas 24 (92%) of 26 cases were hyperintense on T2-weighted sequences. The following enhancement patterns were noted: 6 (38%) of 16 cases revealed homogeneous enhancement (Fig 7C), whereas 5 (31%) of 16 demonstrated heterogeneous enhancement and 3 (19%) of 16 demonstrated only rim enhancement (Fig 5B). One case demonstrated minimal enhancement, whereas another demonstrated no enhancement (Fig 6B).

Of our 26 cases, 17 ependymomas were cellular, 3 were tanycytic, and 6 were myxopapillary. None were epithelial or papillary. T2-weighted images were all very similar regardless of histology subtype, with 24 (92%) of 26 cases hyperintense on T2. Although 18 (90%) of 20 of nonmyxopapillary ependymomas were hypointense or isointense with respect to cord on T1-weighted images and hyperintense on T2-weighted images, we found that 6 (100%) of 6 myxopapillary ependymomas were hyperintense or isointense on both sequences (Fig 7). The signal characteristics ofthe myxopapillary group were significantly different from those of the nonmyxopapillary group, as demonstrated in the Table. Within the nonmyxopapillary subgroup, 90% demonstrated signal characteristics in the isointense or hypointense range on T1-weighted images. However, in the myxopapillary subgroup, 100% demonstrated signal characteristics in the isointense or hyperintense range. Although our number of myxopapillary tumors was relatively small, using the Fisher's Exact test, two-tailed, for data analysis, the signal characteristics of the myxopapillary group were statistically significant ($P = .023$).

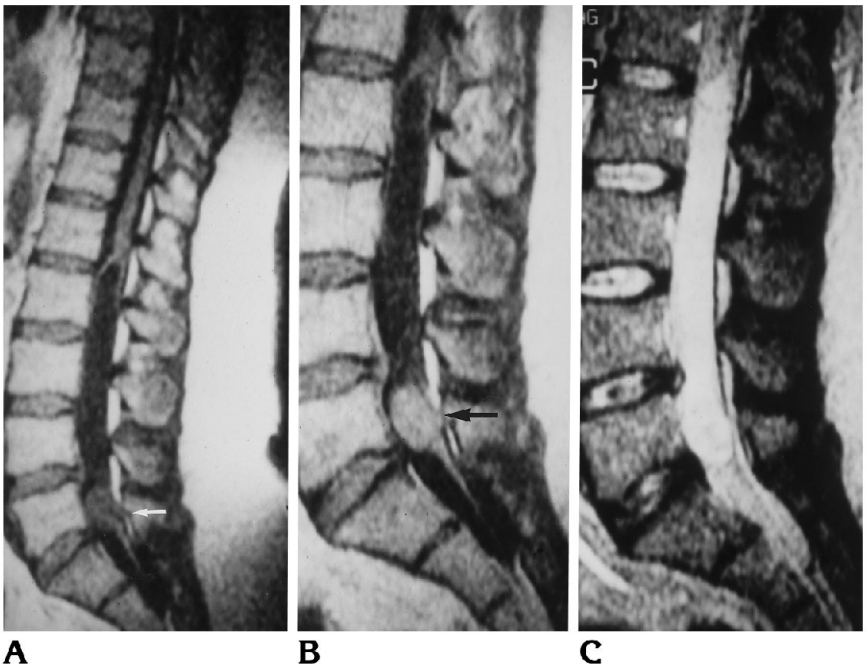

Fig 3. *A*, T1-weighted (400/25/2) sagittal image shows a focal solid, oval-shaped tumor nodule at L-5 (*arrow*), with a long rostral cyst, extending upward to the level of T12-L1. This was a cellular ependymoma.

B, Enhanced T1-weighted (550/25/2) sagittal image demonstrates homogeneous enhancement of the tumor nodule only (*arrow*) and no contrast enhancement around the rostral cyst. At surgery, this rostral cyst was found to contain xanthochromic fluid and no tumor cells.

C, T2-weighted (1800/110/2) sagittal image shows diffuse hyperintense signal within the tumor nodule and adjacent cyst, demonstrating the difficulty of delineating solid from cystic tumoral components on T2-weighted images. Incidental small herniated disk at L4-5.

Discussion

Ependymomas are the most common primary spinal neoplasm of the lower cord, conus, filum, and cauda equina (1), yet relatively few MR-based series have appeared in the literature to explore imaging characteristics.

In our study, in the category of type of cord expansion for cervical and thoracic ependymomas, we obtained expected results. The central location of ependymal cells within the spinal canal explains why many ependymomas grow centrifugally and usually cause symmetric expansion of the cord. This characteristic may help to differentiate them from astrocytomas, which are more-infiltrating neoplasms, and may cause asymmetric, lumpy cord expansion. Our figure of 100% of cervical and thoracic ependymomas causing symmetric cord expansion is compatible with published data (1–3).

Erosive changes are seen commonly in ependymomas, most likely because they are so slow growing. On plain film, it has been reported that 63% of spinal ependymomas show osseous changes at the time of presentation (1). There is often erosion of the medial aspect of the pedicles or scalloping of the posterior surface of the vertebral bodies (4). Osseous erosion and thinning of the pedicles and lamina are far more common in the ependymomas of the lower spinal canal and filum. Our data showed that 11.5% of cases demonstrated osseous abnormality, and in fact, all of our cases that resulted in detectable MR osseous changes were lumbar or lumbosacral tumors. It must be noted that pressure erosion of the spinal canal with flattening of the pedicles is not specific to ependymomas, and may be found in association with several other entities, including astrocytoma (2).

In the next category, the published literature states that 50% of spinal ependymomas will demonstrate associated cysts (1, 5, 6). We found a slightly higher, but essentially compatible incidence of 16 (61.5%) of 26. Three distinct types of cysts have been described: (*a*) tumoral cysts; (*b*) rostral or caudal cysts; and (*c*) reactive dilatation of the central canal. Of our cases with cysts, 50% were intratumoral, 37.5% were rostral or caudal, and 56.3% showed reactive dilatation of the central canal. Some cases contained more than one type of cystic change. There is much debate in the literature, both radiologic and neurosurgical, as to the appropriate nomenclature for cystic changes associated with ependymomas.

When a cyst is seen within the tumor itself, it is known as a true tumoral cyst. This type of cyst is thought to arise from degeneration, necrosis, and liquefaction within the neoplasm (Fig 2). In contains a mixture of differing elements, such as protein, old hemorrhage, and necrotic tumoral tissue (6). This inhomogeneous composition leads to variable signal

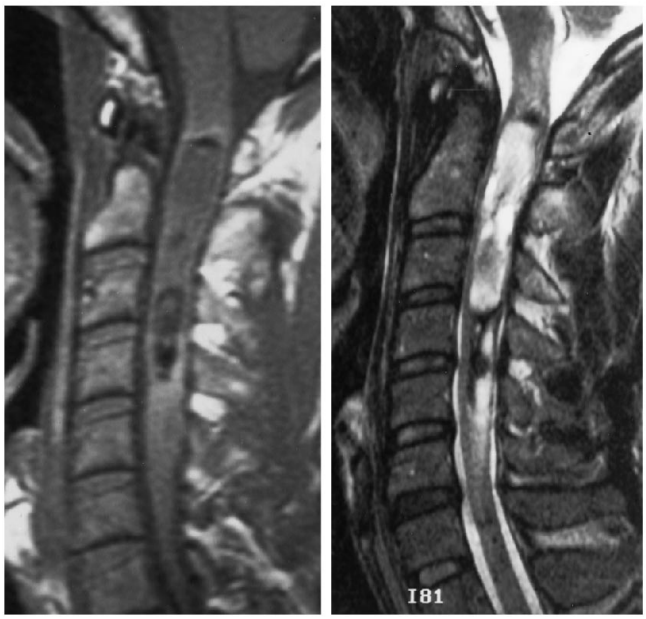

Fig 4. T1-weighted (600/11/2) sagittal image (*A*) and fast spin-echo (4000/102/2) (*B*) demonstrate a cervical cellular ependymoma, with low-intensity hemosiderin both rostrally and caudally on both sequences.

characteristics on MR, and not always the expected low signal intensity on T1 and hyperintensity on T2. Contrast is helpful in identifying these intratumoral cysts because enhancement will be seen around them.

Unlike these true tumoral cysts, the rostral or caudal cysts occur above and/or below the tumor. These cysts do not demonstrate contrast enhancement around their borders, as do the intratumoral cyst (Figs 1 and 3).

The third type of cyst seen in association with spinal tumors is secondary reactive dilatation of the central canal, most likely related to partial obstruction of the central canal by the tumor mass. This central canal dilatation can be recognized because of its central location within the spinal cord, its cerebrospinal fluid–equivalent signal, its location beyond the tumor margins (above and/or below), its lack of enhancement with contrast, and its hypoechoic signal on intraoperative ultrasound. There is resolution of dilatation of the central canal after the removal of the tumor (Fig 1). Distinction between rostral/caudal cysts and reactive dilatation of the central canal may be difficult.

It is important to differentiate tumoral cysts from the other two types of cysts because intratumoral cysts should be surgically excised along with the tumor, because they are intermingled inextricably with the rest of the ependymoma and can be lined with abnormal glial cells, as reported by Goy et al (6). However, rostral and caudal cysts (Fig 3) do not require surgical excision. They may be aspirated and drained, because they are not actually part of the neoplasm itself, but rather a reactive response to it. In fact, rostral and caudal cysts have been shown to contain either hemorrhagic or xanthochromic fluid, but never tumor cells (6, 7).

The preoperative recognition of tumor-associated cysts may be difficult because of their variable signal characteristics; however, it remains an important element of patient care to try to determine what type of cyst is present. The extensive regions of cord enlargement seen on MR may be caused primarily by either long rostral or caudal cysts or by secondary reactive dilatation of the central canal, whereas the tumor itself may be quite small (Fig 3). This knowledge will help the surgeon to plan approach and perhaps limit the length of laminectomy defect. This may reduce the complications of long-term deformity of the spinal column from progressive neurologic dysfunction (6).

It must be noted that the presence of cysts is not specific to ependymomas. Astrocytomas also are characterized by the frequent presence of cystic degeneration reported in approximately 38% of cases. All three types of cystic change may be seen in association with astrocytoma.

With regard to the presence of hemorrhage, 19% of our cases demonstrated detectable evidence of chronic hemosiderin deposition. It is a well-known fact that spinal ependymomas tend to bleed, but the pathogenesis of this occurrence is poorly understood. Both Zimmerman (2) and Li (8) attribute the tendency to hemorrhage to the highly vascular connective tissue stroma. Nemoto (9) postulates that because ependymomas are well circumscribed and lack intervening neural tissue, they are more likely to possess a vulnerable interface between the tumor and normal cord substance, in contradistinction to such tumors as astrocytomas that are poorly defined, infiltrative, and intermingled with neural tissue (9).

Nemoto (9) found that the presence of strikingly hypointense areas on both T1- and T2-weighted images along the tumor margin cor-

Fig 5. T1-weighted (600/20/2) sagittal image (*A*) and corresponding fat-saturated postgadolinium (517/33/2) image (*B*) demonstrate rim enhancement at the inferior margin of a cervical tanycytic ependymoma.

Fig 6. *A*, T1-weighted (550/25/2) sagittal image demonstrates a homogeneous, well-circumscribed, myxopapillary ependymoma at L-2, which is isointense to cord.

B, Postgadolinium (550/25/2) sagittal image shows no enhancement of the tumor nodule. Normal enhancement of the basivertebral plexus at each level is noted.

responds pathologically to a pseudocapsule resulting from old hematoma at the interface between cord and tumor (see Fig 4). His findings led him to conclude that intramedullary tumors with hypointensity at the tumor margins, as described above, were more likely to be ependymomas than other entities such as astrocytomas. This hypointensity at the tumor margins suggests that the tumor is relatively well demarcated from the surrounding spinal cord tissue, as is often the case with ependymomas. As discussed, astrocytomas are more-infiltrative neoplasms, and subsequently are less likely to display the pseudocapsule appearance.

The category of extent of involvement yielded expected results, with an average length of involvement of 4.5 vertebral segments. Zimmerman has previously reported that ependymomas are usually confined to 5 vertebral segments (2), whereas astrocytomas frequently span multiple vertebral segments and often involve the entire spinal cord. If an intramedullary neoplasm involves the total spinal cord, it is more likely to be an astrocytoma (10).

With regard to signal characteristics, overall, our data reflect the generally accepted tenet that ependymomas are isointense to hypointense on T1-weighted sequences and hyperintense on T2. The T1-weighted signal can be either homogeneous or heterogeneous in appearance.

In the remaining category of pattern of enhancement, our study yielded the most unexpected results. Enhancement of ependymomas has been widely reported to show intense, homogeneous, sharply demarcated focal enhancement (3, 11–13). In our study, only 38% of cases reflected this reported enhancement pattern, whereas another 31% demonstrated heterogeneous enhancement. Three cases (19%) demonstrated only rim enhancement, whereas one case demonstrated minimal enhancement, and another demonstrated no enhancement. These latter three enhancement patterns (rim, minimal, and no enhancement) are certainly not well documented in the literature. Overall, in our series, 62% of cases demonstrated one of these previously undocumented enhancement patterns, and because of our large sample size, one can assume that this appearance occurs much more frequently than previously thought.

To review briefly some pathologic character-

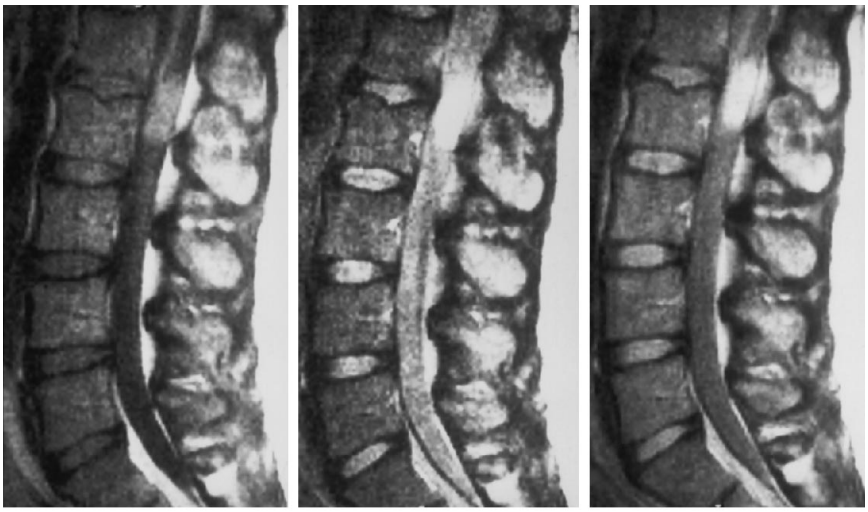

A B C

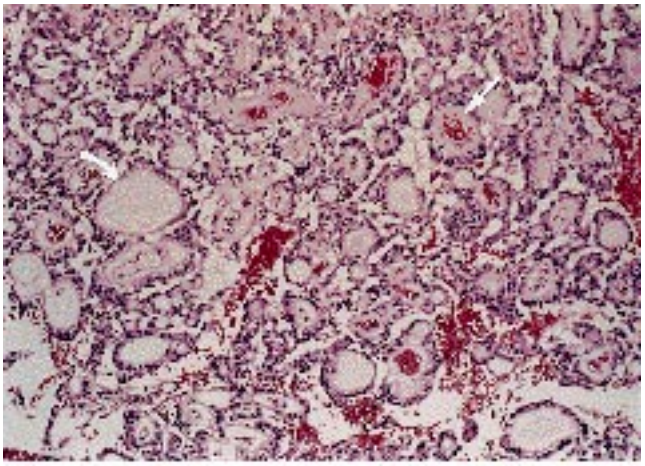

D

Fig 7. *A*, Sagittal T1-weighted image (500/40/2) of a myxopapillary ependymoma at L1-2 demonstrates hyperintense signal.

B, Corresponding T2-weighted (1500/80/2) sagittal image shows homogeneous hyperintensity within the tumor.

C, Enhanced (500/40/2) sagittal image demonstrates homogeneous enhancement of the tumor.

D, Histologic image from this patient shows multiple glandlike or cystic spaces filled with mucin (*curved arrow*) and multiple blood vessels, with a rim of mucin deposited in a perivascular distribution around the walls of the central blood vessels (*straight arrow*) (hematoxylin-eosin stain, magnification ×250).

Signal intensity on T1-weighted images

Intensity	Myxopapillary (n = 6)	Nonmyxopapillary (n = 20)
Hypointense	0 (0%)	13 (65%)
Isointense	2 (33.3%)	5 (25%)
Hyperintense	4 (66.7%)	2 (10%)

istics of spinal ependymomas, ependymomas are classified into five main histologic types: cellular, papillary, epithelial, tanyctic, and myxopapillary (14). Cellular ependymoma is by far the most common subtype. It is composed of cuboidal or low columnar cells arranged in a diffuse fashion. A special histologic characteristic that helps to distinguish these tumors is the perivascular pseudorosette formation in which clear tumor cells align themselves in a ring around blood vessels (14) (see Fig 1E). The papillary subtype of ependymoma is a relatively rare variant. It is very similar histologically to choroid plexus papilloma. Both frequent the ventricles, but only papillary ependymomas contain a glial stroma within a papillary core. The epithelial subtype is charactertized by specific cellular surface arrangements that may be either linear or closed to form glands or canals (14). These glands are referred to as true ependymal rosettes in distinction to the perivascular pseudorosettes found in the cellular type. The tanycytic ependymomas are composed of elongated cells similar in appearance to astrocytoma. These highly fibrillary tumors lack the true-ependymal rosettes, and the perivascular pseudorosettes are remarkable inconspicuous.

The myxopapillary ependymoma subtype arises almost exclusively from the filum terminale. They represent 27% to 30% of all ependymomas (15). Most occur in the fourth decade of life. These tumors usually appear as a round or sausage-shaped mass in the filum, sometimes involving the conus. They often are encapsulated and may be tethered both proximally and distally. Smaller tumors tend to displace the nerve roots of the cauda equina, whereas the large tumors often compress or encase them.

This particular subtype is also the variant most prone to hemorrhage. In fact, they have been known to present occasionally as subarachnoid bleed. When this occurs, the MR appearance is one of superficial siderosis of the subarachnoid space, dramatically outlining the brain stem, cisterns, fissures, and all surfaces of the brain. This phenomenon is caused by the deposition of iron pigments on the pial and arachnoidal surfaces (2).

Myxopapillary tumors are unique for their intracellular and perivascular accumulation of mucin (see Fig 7). Mucin, which is proteinaceous, should be hyperintense on both T1- and T2-weighted sequences (15). When present within the connective tissue elements, mucin may demonstrate specific signal characteristics, suggesting the diagnosis of myxopapillary variant. This is the only ependymoma subtype with histologic characteristics likely to distinguish itself on MR imaging, and our results supported this hypothesis. In our study, we found the myxopapillary variant demonstrated unique imaging characteristics on T1-weighted sequences, probably as a result of the mucin accumulation. The MR characteristics of mucin would explain our findings that a statistically significant percentage of myxopapillary subtypes are somewhat hyperintense on both T1- and T2-weighted sequences, whereas nonmyxopapillary ependymoma subtypes are isointense to hypointense on T1.

The presurgical differentiation between ependymomas and astrocytomas is beneficial to the surgeon for operative planning. Ependymomas are usually well circumscribed and relatively amenable to complete removal, whereas the more infiltrative astrocytoma is much more difficult to excise totally (9). The compiled list of MR characteristics of ependymomas may help the radiologist in suggesting this distinction preoperatively. Our findings regarding histopathologic correlation show that myxopapillary ependymomas demonstrate distinct signal characteristics on T1-weighted images, probably because of the accumulation of mucin. If one encounters a tumor in the filum with hyperintense signal on T1, there is a high probability that it is a myxopapillary ependymoma. Our findings regarding enhancement patterns are quite different from the reported literature, but we feel that this may be because our series is larger than those previously reported. Recognition of these varied types of enhancement should prove useful for diagnosis.

Acknowledgments

Special acknowledgment goes to Judith Bean, PhD, for her help with the statistical analysis and Jean Alli for help with secretarial assistance.

References

1. Atlas S. *Magnetic Resonance Imaging of the Brain and Spine*. 1991:956–958
2. Zimmerman R, Bilaniuk L. Imaging of tumors of the spinal canal and cord. *Radiol Clin North Am* 1988;26(suppl 5):965–1007
3. Epstein F, Farmer JP, Freed D. Adult intramedullary spinal cord ependymomas; the result of surgery in 38 patients. *J Neurosurg* 1993;79:204–209
4. Lombardi G, Passerini A. *Spinal Cord Disease, a Radiologic and Myelographic Analysis*. Baltimore: Williams and Wilkins, 1964
5. Slasky BS, Bydder GM, Niendorf HP, Young IR. MR imaging with gadolinium-DTPA in the differentiation of tumor, syrinx, and cyst of the spinal cord. *J Comput Assist Tomogr* 1987;11:845–850
6. Goy A, Pinto R, Raghavendra B, Epstein F, Kricheff I. Intramedullary spinal cord tumors: MR imaging with emphasis on associated cysts. *Radiology* 1986;161:381–386
7. McCormick P, Torres R, Post KD, Stein BM. Intramedullary ependymoma of the spinal cord. *J Neurosurg* 1990;72:523–532
8. Li M, Holtas S. MR imaging of spinal intramedullary tumors. *Acta Radiol* 1991;32:505–513
9. Nemoto Y, Inoue Y, Tashior T, et al. Intramedullary spinal cord tumors: significance of associated hemorrhage at MR imaging. *Radiology* 1992;182:793–796
10. Scotti GM, Scialfa G, Colombo N, Landona L. Magnetic resonance diagnosis of intramedullary tumors of the spinal cord. *Neuroradiology* 1987;29:130–135
11. Parizel P, Baleriaux D, Rodesch G, et al. Gd-DTPA-enhanced MR imaging of spinal tumors. *AJNR Am J Neuroradiol* 1989;10:249–258
12. Ferrante L, Mastronardi L, Celli P, et al. Intramedullary spinal cord ependymomas: a study of 45 cases with long-term follow-up *Acta Neurochir* 1992;119:74–79
13. Rothwell CM, Jaspan T, et al. Gadolinium-enhanced magnetic resonance imaging of spinal tumors. *Br J Radiol* 1989;62:1067–1074
14. Burger P, Scheithauer B, Vogel FS. *Surgical Pathology of the Nervous System and Its Coverings*. 3rd ed. 1991:271–283
15. Wagle W, Jaufman B, Mincy JE. Intradural extramedullary ependymoma: MR pathologic correlation. *J Comput Assist Tomogr* 1988;12(suppl 4):705–707